Electronic Supplementary Material (ESI) for Nanoscale.

Supporting Material

.

Correlative AFM and fluorescence imaging demonstrate nanoscale membrane remodeling and ring-like and tubular structure formation by Septins

Anthony Vial, Cyntia Taveneau, Luca Costa, Brieuc Chauvin, Hussein Nasrallah, Cédric Godefroy, Patrice Dosset, Hervé Isambert, Kien Xuan Ngo, Stéphanie Mangenot, Daniel Levy, Aurélie Bertin, Pierre-Emmanuel Milhiet

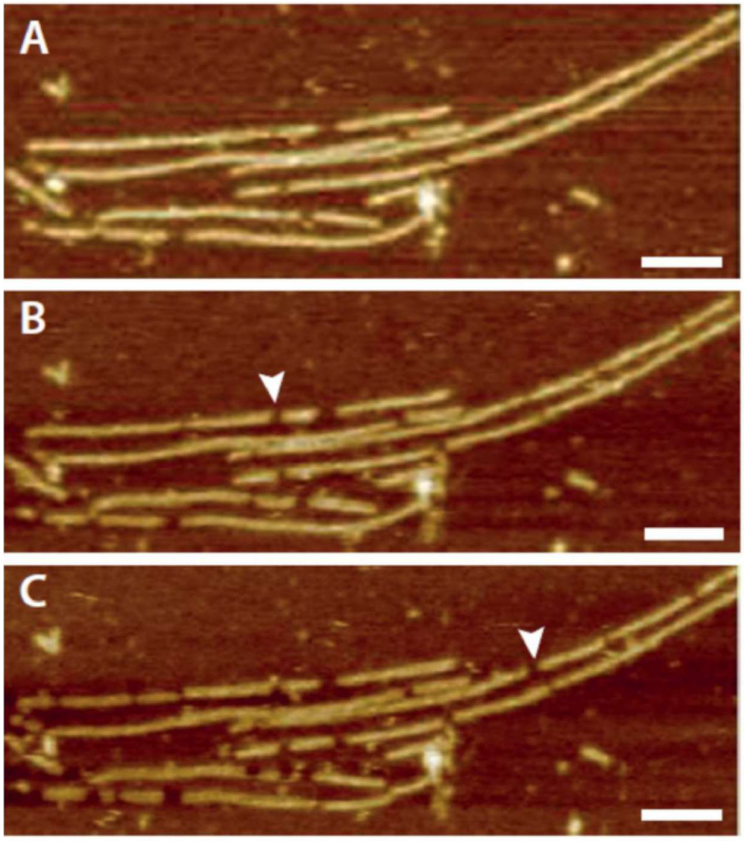

Supplementary Figure 1. AFM imaging of septin filaments coated on mica
A, B and C are successive AFM height images recorded in liquid at low density. The white arrows indicate a gap of ~20 nm in the filament corresponding to the removal of septin, illustrating filament sensitivity to tip scanning. Scale bar, 100 nm; z scale 10 nm.

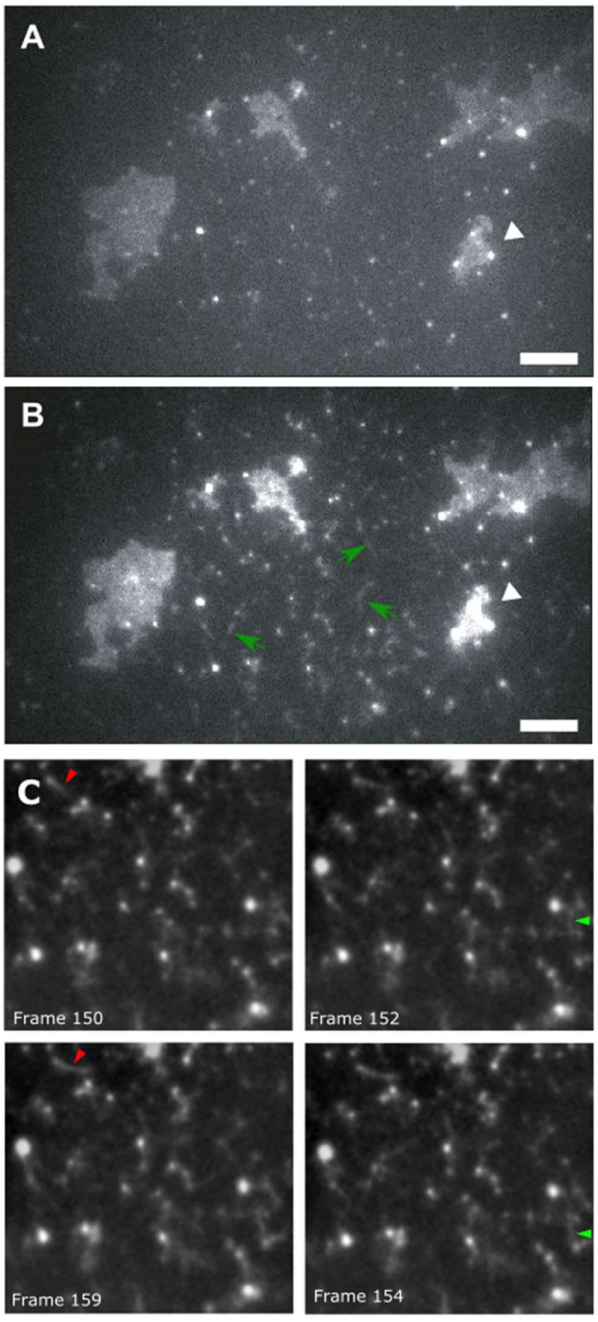

Figure S2 – Fluorescence widefield TIRF images of supported lipid membranes incubated with 80 nM septin

Fluorescence imaging of SLB composed of POPC, POPE, POPS, PIP2 at 50:35:10:5 ratios incubated with GFP-septin and observed using TIRF microscopy, just after the addition of septin (A) or 7 min after (B). The white arrowheads in A and B highlight the change in intensity between the two times of incubation showing accumulation of septins over time; the green arrows indicate filamentous structures. C: snapshots of Movie 2 showing that some filaments appeared to be attached only by one end (see red or green arrowheads for comparison of the position of filaments in different frames). Scale bar, 5 µm. See the corresponding movie (Movie 2) described below.

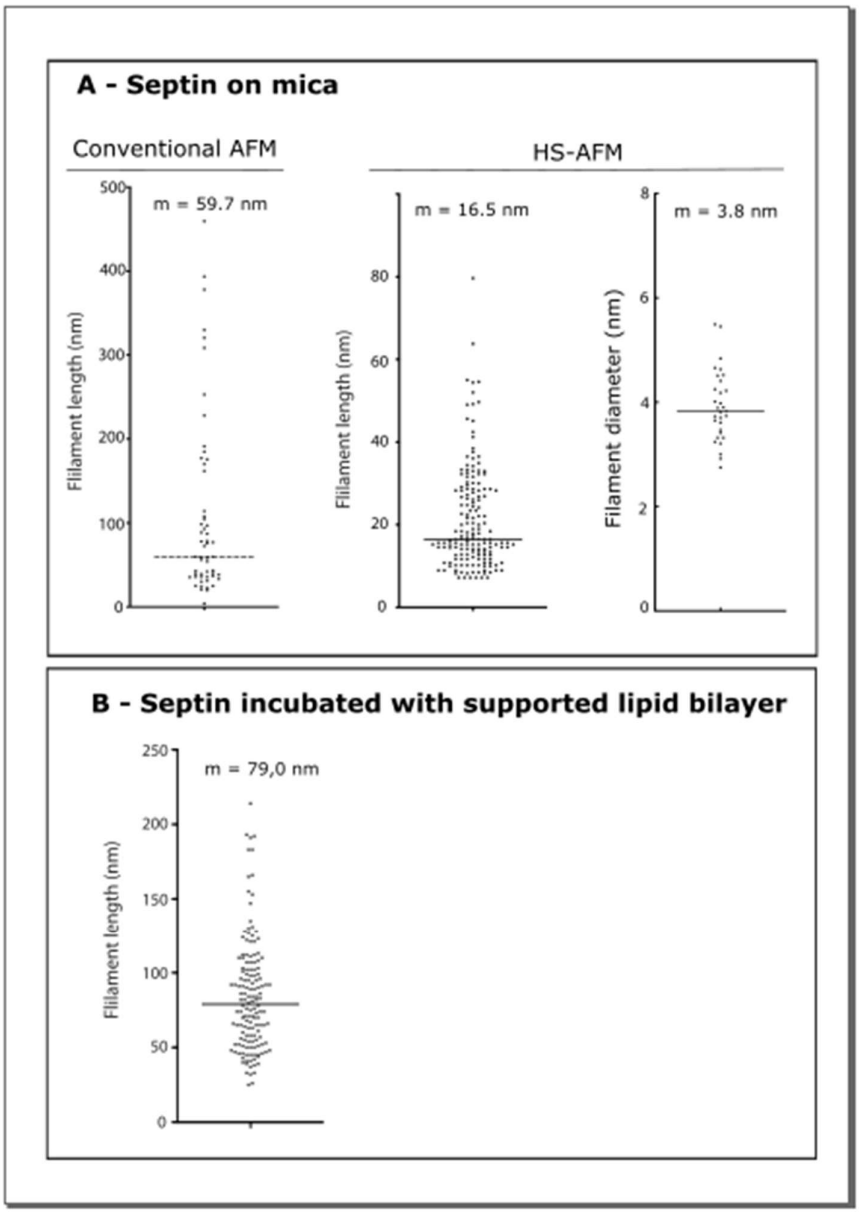

Figure S3 - Analysis of septin length and diameter in low salt concentration

All the measurements are represented as scatter plots and the median value is indicated at the top of each graph.

Panel A: Scatter plots of the length and diameter values of septin on mica measured from height images (see Figure 1). The left panel corresponds to septin filaments that have been formed in low salt concentration solution and then coated on mica and imaged in liquid using conventional AFM. The right panel corresponds to HS-AFM experiments where septin and its oligomerization were observed in real time in liquid. The diameter was estimated by measuring the height as compared to mica to avoid the contribution of tip convolution.

Panel B: Scatter plot of septin length value measured from 5 different areas when 80 nM of the protein was incubated in low salt buffer with supported lipid bilayers composed of EPC, DOPE, DOPS, Chl, PIP2 at 55:10:10:15:10 ratios and were observed using HS-AFM (Figure 3B and 3C).

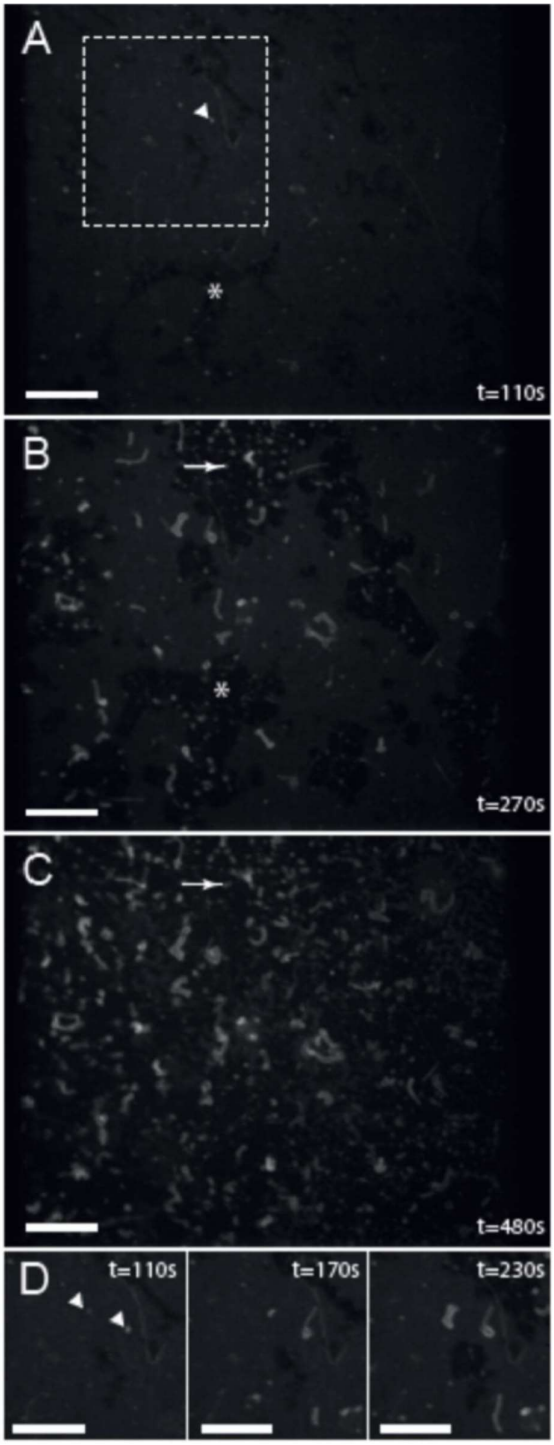

Figure S4 -Fluorescence widefield TIRF images of supported lipid membranes incubated with 300 nM septin

Fluorescence imaging of SLB composed of EPC, DOPE, DOPS, Chl, PIP2 at 55:10:10:15:10 ratios incubated with GFP-septin and observed using TIRF microscopy, after incubation with septin for 110s (A), 270 s (B) and 480s (C). The asterisk indicates mica (non-fluorescent), the white arrowhead points out a septin cluster and the white arrow indicates a ring-like structure that can be better observed in Figure 4C. D corresponds to shortest time intervals of the area indicated in A by a white dotted line, demonstrating that tubes started arising from a septin cluster (white arrowheads). Scale bar, 20 µm. See the corresponding movie (Movie 6) described below.

Movie 1 – HS-AFM imaging of purified septin coated on mica
Septin were imaged in low salt buffer and HS-AFM height images were recorded in liquid at 1 frame/s. See snapshots in Fig. 1C. The movie was drift corrected using the software WSxM[1] and accelerated 3 times. Scan of 600 nm.

Movie 2 – TIRF fluorescence imaging of supported lipid bilayer incubated with GFP-septin
Widefield TIRF fluorescence movie of SLB composed of POPC, POPE, POPS, PIP2 at50:35:10:5 ratios (the field width is 49.8 µm). The total duration of the movie is 13.3 min recorded at 1 frame every 5 s. The brighter areas correspond to septin bound to mica as shown in Figure 2. The surface of theseseptin-enriched areas increases over time and also becomes brighter, indicating both membraneremodeling and 3D stacking of septin. Formation of filamentous structures of up to 2.5 µm in length is also observed over time. Many of them appeared to be attached to the membrane through a single anchoring point, with the rest of the filament floating in the buffer.

Movie 3 - HS-AFM imaging of supported lipid bilayer incubated with septin
HS-AFM movie of SLB composed of EPC, DOPE, DOPS, Chl, PIP2 at 55:10:10:15:10 observed using HSAFM just after the addition of 80 nM septin in low salt buffer (<15 min incubation). The movie displays height images (see a snapshot in Fig. 3A) and was recorded at 1 image/s (scan of 800 nm). Roundshaped dynamic septin assemblies were observed, directly interacting with mica and protruding 2 to 5 nm above the mica and displaying a diameter of 10 nm. Similar assemblies were also observed at thesurface of the lipid bilayer, protruding up to 10 nm above the membrane, as well as larger patchesprotruding ~ 2 nm above the membrane that appeared to be very dynamic as shown by the diffusion within the patch.

Movies 4 and 5 – Membrane destabilization by septins imaged by AFM
This HS-AFM movie illustrates the ability of septin oligomerization to destabilize SLB composed of EPC,DOPE, DOPS, Chl, PIP2 at 55:10:10:15:10 ratios. Height images were recorded at 1 image/s (scan of 400 nm) in low salt conditions. Filaments at the top of mica were clearly observed (see a snapshot in Fig. 3B). The length of these filaments varied, from a few tens to a few hundreds of nanometers. We could observe the Brownian movement of these filaments. In Movie 4, the bright dot probably corresponds to a membrane patch that can be used as a fiducial mark, allowing for the subtraction of drift during imaging. In Movie 5, the black frame indicates a time lapse of 2 min.

Movie 6 - Septin-induced reshaping of membrane forms doughnut-shaped structures
HS-AFM imaging of SLB composed of POPC, POPE, POPS, and PIP2 at 50:35:10:5 ratios after 60 min of incubation with 80 nM septin. HS-AFM allows for real-time capture of the spontaneous formation of doughnut-shaped structures from the 2D lipid bilayer organization (see snapshots in Fig. 4A). The membrane reshaped to produce a ring shape of 1.1 µm diameter and 10-20 nm thickness within a few tens of seconds. Height images were recorded at 1 image/s (2 µm scan).

Movie 7 - Formation of membrane tubes from supported membranes induced by septin.
Fluorescence imaging of membranes composed of EPC, DOPE, DOPS, Chl, PIP2 at 55:10:10:15:10 ratios supplemented with 0.1% GloPIP Bodipy C16 incubated with 300 nM septin and observed using confocal microscopy (see snapshots of this movie in Fig. 5). Immediately upon septin addition, a few thin and long filaments were observed and the lipid bilayer appeared highly disrupted with holes, leaving bare the surface of mica (black areas). Septins accumulated at the lipid bilayer-mica interfaces and tubes started arising from the surface of the bilayer, generally from a septin cluster. The movie corresponds to a 150*112 µm field of view. The total duration of the movie is 20 min recorded at 1 frame every 10 s.

Movie 8 - Septin sensitivity to AFM tip scanning
Fluorescence image of GFP-septin in interaction with a SLB composed of EPC, DOPE, DOPS, Chl, PIP2 at 55:10:10:15:10 ratios, incubated with 80 nM septin and recorded with a correlative fluorescence- HS-AFM microscope[2]. This movie highlights the fragility of septin filaments to forces applied by the AFM tip by recording in real time both the fluorescence of GFP-septin and sample topography. Upon scanning the fluorescence disappeared but the AFM image showed that the lipid bilayer was not disrupted during tip

scanning (data not shown). The movie corresponds to a wide-field optical image recorded with an inverted microscope equipped with an EM-CCD camera. 500 nm AFM scans were recorded at 1 frame/s at different positions. The movie is accelerated 5 times.

References

1 I. Horcas, R. Fernández, J. M. Gómez-Rodríguez, J. Colchero, J. Gómez-Herrero and A. M. Baro, *Rev Sci Instrum*, 2007, **78**, 013705.

2 S. Fukuda, T. Uchihashi, R. Iino, Y. Okazaki, M. Yoshida, K. Igarashi and T. Ando, *Rev Sci Instrum*, 2013, **84**, 073706.